THD analysis and small AC signal analysis of trans-Z-source and quasi-Z-source inverter for linear and non-linear load

Manish Bharat[1,3], ASR Murty[2], Ritesh Dash[1]
[1]School of Electrical and Electronics Engineering, REVA University, Bengaluru, India
[2]Department of Electrical and Electronics Engineering, Rajarajeswari College of Engineering, Bengaluru, India
[3]Department of Electrical and Electronics Engineering, Visvesvaraya Technological University, Belagavi, India

Article Info	ABSTRACT
  	The paper primarily focuses on the ongoing research related to Z source inverter technologies (ZSITs) used in the transportation industry, particularly for electric vehicles (EVs) and hybrid electrical vehicles (HEVs). It analyzes various topologies of ZSITs based on their mode of operation, capacitor voltage stress during active states and non-active state operations, DC link voltage before inverter module and line to line output voltage across the load. The paper compares the conventional trans-z source and two port quasi-Z source inverter model networks for multiple parameters and derives mathematical equations for both linear and non-linear loads. Practical and theoretical calculations match when using a modulation index of M=0.85 and a duty ratio of 1.414. The result obtained in this paper indicates that the proposed solution is better in terms of reduction in total total harmonics distortions (THD) percentage of 18.14% during the transition condition. All the analysis has been carried out with MATLAB based Simulink model. *This is an open access article under the <ins>CC BY-SA</ins> license.*

Corresponding Author:

Manish Bharat
School of Electrical and Electronics Engineering, REVA University
Bengaluru, India
Email: manishb87@gmail.com

1. INTRODUCTION

As the demand for clean and sustainable electricity continues to increase, the adoption of renewable energy sources such as solar and wind power has become increasingly popular. Studies suggest that solar photovoltaic (SPV) systems are a promising solution for meeting current energy demands worldwide. However, the inverter plays a critical role in SPV generation, and traditional methods of increasing voltage levels using DC-DC boost converters or transformers can result in higher power losses and increased costs for the entire system. Moreover, additional conversion stages can decrease the overall efficiency of the system.

The use of a Z-source inverter (ZSI) is beneficial in achieving a significant voltage step change during a single-stage conversion process by introducing a high impedance network before the voltage source inverter (VSI) circuit. Many topologies have been explored in this field, and the paper proposes a cost-effective and efficient modified boost topology for an impedance source inverter that incurs low voltage loss. The quasi-Z-source inverter (q-ZSI) is analyzed in detail in reference to [1], [2], which provide a comprehensive derivation and analysis of ZSI, showcasing different configurations while retaining the same operating principle. The q-ZSI provides several advantages, such as lower device rating, no requirement for filtering capacitors, less switching interval ripples, and the maintenance of a constant DC ripple-free input current to the inverter circuit from SPV sources [3], [4]. Qian *et al.* [5] proposes a unique q-ZSI topology that can boost voltage and minimize current ripple. This is achieved through the utilization of two switched impedance networks and a modified pulse width modulation (PWM) technique to control the inverter's output voltage. The authors

performed simulations and experiments to evaluate the performance of the proposed topology in terms of voltage boosting, current ripple reduction, and efficiency. The outcomes confirm that q-ZSI can effectively enhance the output voltage while reducing the current ripple, which makes it a potential solution for renewable energy applications.

An electric vehicle (EV) is composed of various components, including motors, battery, battery management system, DC to DC converter, and DC to AC converter, working together to transmit power from the battery to the electric motors. Precise parameter settings are essential in EVs because power electronic components and switches require accurate frequency control for smooth and uninterrupted operation. To reduce overall costs, synchronous and induction motors are typically used in EVs, with induction motors offering speed control over a wide range with minimal time required, a simple and robust DC to AC converter design, and lower maintenance costs [6]. Yuan *et al.* [7] presents an analysis of the small signal modeling and transient behavior of a trans quasi-Z-source inverter (TqZSI), which is a modified version of the qZSI. The TqZSI, while having a higher number of components than the qZSI, can achieve better voltage boosting and current ripple reduction. The authors develop a state-space averaged model of the TqZSI and use it to analyze the inverter's small-signal stability, harmonic distortion, and transient response. The simulation results indicate that the TqZSI exhibits better voltage regulation and transient response compared to the qZSI, making it a potential candidate for use in renewable energy applications.

The paper highlights the significance of regenerative braking in induction motors used in EVs particularly in situations where high torque and power are required, such as hill climbing and emergency braking. The authors stress the importance of achieving high efficiency in the conversion ratio for effective regenerative braking in EV induction motors. References [7], [8] are cited as sources of information regarding this matter. Guo *et al.* [9], proposes a new method for optimizing torque ripple reduction in direct torque control (DTC) using a multilevel inverter. The method utilizes a cost function based on Fourier coefficients of the torque ripple waveform to evaluate different voltage vectors and finds the optimal combination of voltage vectors through a genetic algorithm. Simulation results indicate that the proposed method is effective in reducing torque ripple and improves performance compared to conventional DTC methods.

Torkaman *et al.* [10] introduction to batteries and battery management systems (BMS) utilized in EVs. The authors examine different battery types like nickel-metal hydride, lead-acid and lithium-ion batteries and compare their attributes regarding energy density, power density, cost, and safety. The paper also covers the difficulties and opportunities of battery management, including state-of-charge and state-of-health assessment, thermal management, and cell balancing. In conclusion, the article discusses the future trends and potential of batteries and BMS in the EV sector.

Most of the EV's are powered through the DC battery sources as well as fuel cells for achieving the high power for three phase induction motor. The converters circuits are used to convert DC power to the AC power before feeding to the three-phase induction motor. During the vehicle running action which consists of acceleration, deacceleration and breaking, a huge variation occurs in the current, which terns leads in the switching stress of the insulated gate bipolar transistor (IGBT's). The charging and discharging cycle of DC battery depends on the voltage stress across the IGBT's.

Various PWM techniques are discussed which are used to reduce the voltage stress across the IGBT's switches [11]. A graphical comparison of voltage, current, speed and torque is shown in paper [12]. The selection of DC battery is based on the above mention literature survey.

In the above said literature survey analysis, it is understood that the Z source inverter requires precise voltage across its input to either perform the boost or buck operation [13]. The involvement of high frequency components in the Z source inverter may result into the electromagnetic interference with the control system of motors employed in EV's. Another problem that often arrives in EV system is, during acceleration and deacceleration, the switching stress also increases in the system. Although the Z source inverter is known for its capacity in handling the voltage fluctuation at the input of inverter. However, the poor switching handling capacity makes it not suitable for EV related applications. Another major problem with ZSI is the battery management system. The charging and discharging pattern of battery particularly used in EV requires high switching operation with may results into poor management system.

In this paper small AC signal modelling of Z-source inverter, trans-z source and two qZSI for a load of 5 kW induction motor with a DC input of 100 V is modelled. The DC link voltage is boosted before feeding to the three-phase converter circuit using two inductors and two capacitors in X shape. SPWM methods are used to generate 9 different pulses for S_1 to S_9 in the MATLAB/Simulink software. All the three inverter models are connected to the induction motor and the total harmonic distribution is calculated and compared. All three models exhibit single conversion technique to boost the input DC voltage to the power converter circuit [14], [15].

In the continuation to the above remarks about the literature survey and research gap, the following notable work has been carried out this research article.

− A comparative analysis about the two-port quasi Z source inverter and other classical Z source inverter in terms of THD level has been presented [16].
− A two trans Z source network with neural back up along with PWM technique has been proposed and demonstrated with two different state variables [17].
− Both online and offline mode of duty cycle evolution has been presented in order to reduce the switching losses occurring in PWM inverter [18].

2.   PROBLEM FORMULATION AND SOLUTION METHODOLOGY

One of the major disadvantages of EVs is the long range distance coverage because of limited battery backup. Most of DC-DC converters as unable to solve the issue due to different problems arises in maintaining the batter state of charge (SoC). In 2003, Peng [19] discovered a topology known as ZSIT which has lot of advantage over the various multi-port DC-DC converters. This topology helps in boosting the DC voltage without any extra circuit and provides efficient voltage to drive single phase and three phase AC motors [19], [20].

To control the output voltages across the load inverters uses various pulse width modulation techniques i.e simple boost control method, maximum boost control method and maximum boost constant control method [21]. Most of the ZSIT topology uses simple boost control method to generate pulse for three phase inverter. Sine wave is compared with the triangular wave to generate pulses. In this research reference wave of 50 Hz is compared with the triangular wave of 10 Khz is used to produce gating pulse. These pulse are given to the switches S1 to S6 in alternate way to produce maximum output voltage with constant modulation index and variable duty cycle [22].

Modified trans-ZSIT having switch the input side which provides protection from rate of change of high voltage and current. Two inductors are mutually coupled and provide isolation to the circuit presented in Figure 1. The revised impedance network of this inverter has eliminated shoot through obstacles. Transformers and connected inductors raise the circuit's cost.
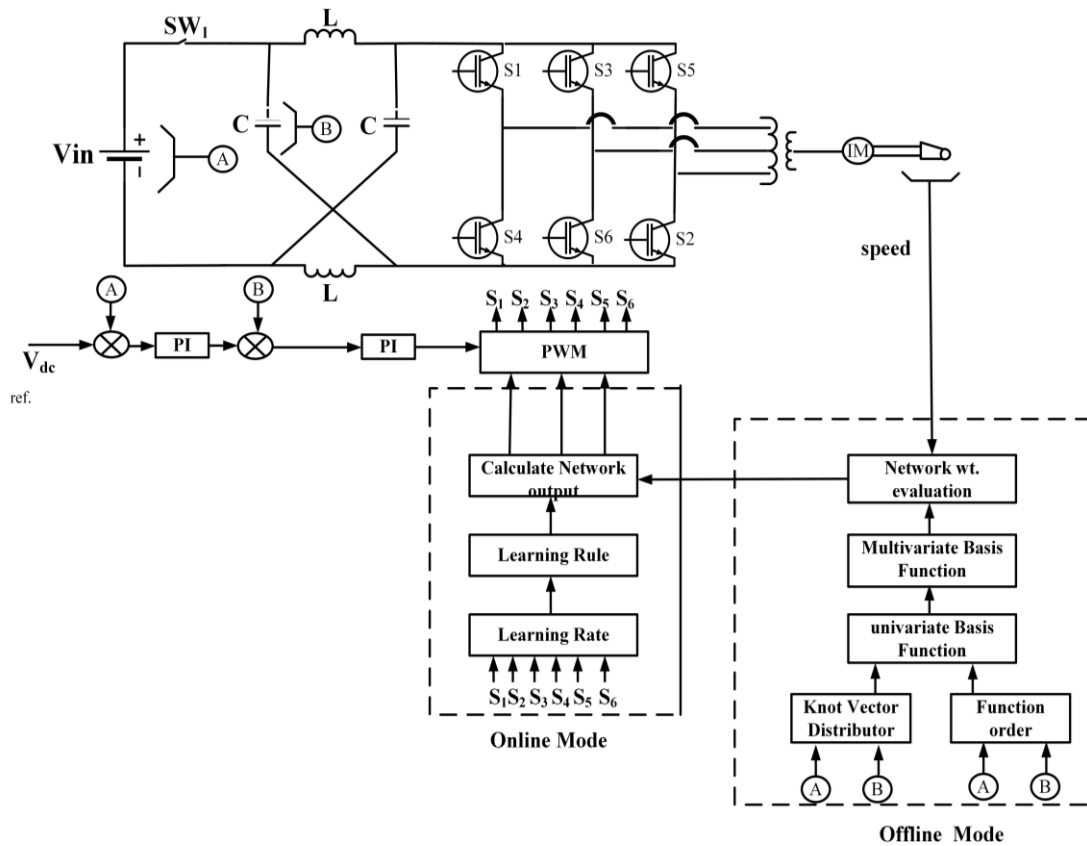

Figure 1. Two trans Z source network with neural connection

Any inverter's performance is entirely dependent on an effective and dependable control technique. It is acknowledged that Z-source inverters with modifications can be used in driving applications for electric and hybrid vehicles. The impedance network modification and control methods used in Z-source inverters are reviewed, and the specifics are described in the following paragraphs. From the Figure 2, the output voltage equations are derived form shoot through and non-shoot through modes of operation.

Shoot-through state

$$V_{L1} = V_{L2} + V_{C1} + V_{DC};$$

$$V_{L2} = \frac{V_{C1}}{\gamma_T - 1} \tag{1}$$

Non-shoot-through state:

$$V_{L2} = -V_{C1}; V_{L1} = \gamma_T * V_{L2} \tag{2}$$

Capacitor voltage:

$$V_C = \frac{\left(\frac{D_{ST}}{\gamma_T - 1}\right) * V_{DC}}{\left(1 - \left(1 + \frac{1}{\gamma_T - 1}\right)D_{ST}\right)} \tag{3}$$

DC link voltage:

$$V_i = \frac{V_{DC}}{\left(1 - \left(1 + \frac{1}{\Gamma - 1}\right)D_{ST}\right)} \tag{4}$$

AC RMS voltage:

$$V_{ac} = \frac{0.5 * M * V_{DC}}{\left(1 - \left(1 + \frac{1}{\gamma_T - 1}\right)D_{ST}\right)} \tag{5}$$
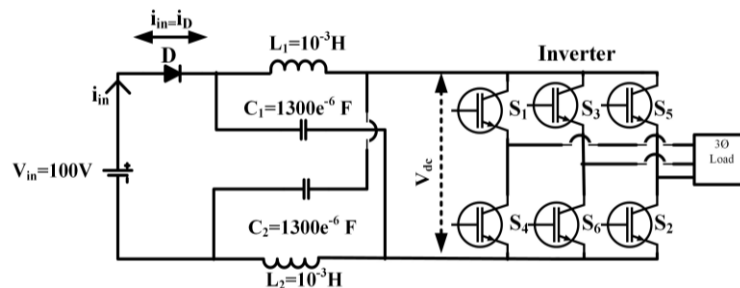

Figure 2. 3-phase traditional ZSIT [3]

The classical ZSI using PWM control technique uses two inductor, two capacitor and 6 number of IGBT's switches to convert 100 V input to 97 V AC in the buck conversion mode. The particular setup has produced an output with that of THD level of 5.42% and 6.43% with the a linear and non-linear load with an DC input supply of 100 V [23]. To boost the input voltage, a capacitor of 22.7 uF is implemented with an inductor value of 160 uH. However, from the EV prospective point of view maximum boost control technique (MBCT) is superior as compare to PWM based techniques in terms of reducing THD content to 38.64% with a line current of 0.15 A. The reduction in the line current also have an negative impact on the torque produced by the three phase IM, there by resulting in the reduction of motor speed [24], [25].

With respect to maximum constant boost control technique (MCBCT) it is observed the line current can be increase to 24 A with an output voltage of 400 V AC. This requires a DC link voltage of 398 V (unstable) due to charge in switching frequency. The setup also produces a THD level of 55.65%. The increase in the line current requires a precession battery management system along with necessary cooling architecture use in order to safe guard the battery. Therefore, it is proposed to reduce the line current to 5.2 A with an voltage 280 V as per Figure 1 [26].

3. SMALL SIGNAL AC MODELLING OF ZSI TOPOLOGY

ZSIT, as shown in Figure 2, it consist of a DC source, zig zag impedance network two coupled capacitance (C1, C2) and inductors namely (L1, L2). Its works in two different stages (a) initial state and (b) non initial state as represented in Figures 3(a) and (b) [27].

Because of the symmetry of the Z-source inverter, the parameters $L_1=L_2=L$ and $C_1=C_2=C$ are both equivalent.

$$T = T_1 + T_0 \tag{6}$$

Figure 3(b) shows that during active mode, the capacitors are charging and the inductors are discharging. Voltages are mathematically derived using KVL inside the loop:

$$V_{dc} = V_{in} + V_C - V_L \tag{6a}$$

$$V_L = -V_C \tag{6b}$$

$$V_{dc} = V_{in} + 2V_C \tag{7}$$
$$V_{in} - V_C - V_L = 0 \tag{8}$$

$$V_L = V_{in} - V_C$$

$$V_{dc} = 0 \tag{9}$$
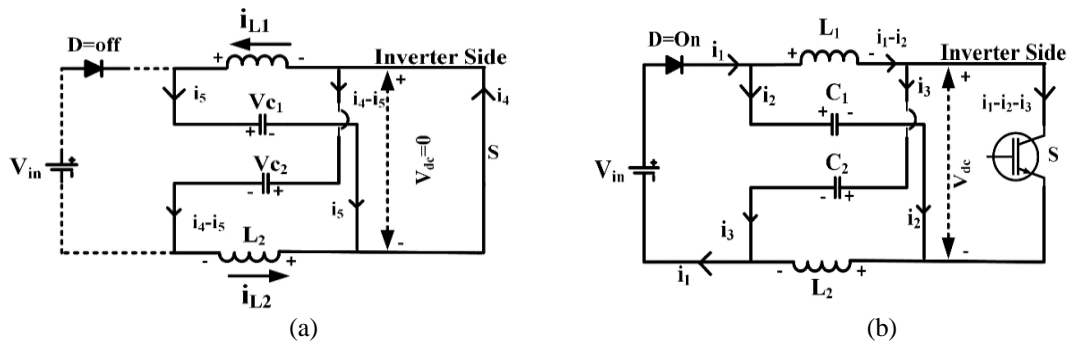
Figure 3. ZSIT two modes of operation; (a) initial state and (b) non-inital state

The voltage equation during the shoot through and non shoot through states are:

$$\frac{1}{T}\int_0^T V_L(t)dt = \frac{T_{st}V_C + T_1(V_{in}-V_C)}{T} = 0 \tag{10}$$

From (10):

$$\frac{V_C}{V_{in}} = \frac{T_1}{T_1 - T_{st}} = \frac{1-D_{st}}{1-2D_{st}} \tag{11}$$

From (11):

$$D_{st} = \frac{V_C - V_{in}}{2V_C - V_{in}} \tag{12}$$

$$D_{st} = \frac{T_{st}}{T}$$

From (7) and (11), Vdc equal to:

$$V_{dc} = \frac{T}{T_1 - T_{st}}V_{in} \tag{13}$$

From (13) can also be expressed as (14):

$$V_{dc} = \frac{1}{1-2D_{st}}V_{in} = BV_{in} \tag{14}$$

3.1. Z-source small signal modelling

As shown in Figures 3(a) and (b), this circuit comprises of two switching states that are dependent on two switches, S_1 and S_2. When S_1 is "on" and S_2 is "off", the first switching state, known as the active state, occurs.

In the two different modes of operation the energy flow from source to load during non shoot through and load to source during shoot through state. In this condition, the DC voltage source and the load are separated, and the ZSI capacitances are charging the ZSI inductances, so no energy is transferred from the DC voltage source to the load. The switching interval S_2 determines the shoot-through duty ratio D1.

$$x(t) = [i_{L1}(t)\ i_{L2}(t)v_{c1}(t)v_{c2}(t)i_{load}(t)]^T \tag{15}$$

$$\begin{bmatrix} L_1 & 0 & 0 & 0 & 0 \\ 0 & L_2 & 0 & 0 & 0 \\ 0 & 0 & C_1 & 0 & 0 \\ 0 & 0 & 0 & C_2 & 0 \\ 0 & 0 & 0 & 0 & l_{load} \end{bmatrix} \nabla \begin{bmatrix} i_{L1}(t) \\ i_{L2}(t) \\ v_{c1}(t) \\ v_{c2}(t) \\ v_{c2}(t) \end{bmatrix} = \begin{bmatrix} 0 & 0 & 1 & 0 & 0 \\ 0 & 0 & 0 & 1 & 0 \\ -1 & 0 & 0 & 0 & 0 \\ 0 & -1 & 0 & 0 & 0 \\ 0 & 0 & 0 & 0 & -R_{load} \end{bmatrix} \begin{bmatrix} i_{L1}(t) \\ i_{L2}(t) \\ v_{c1}(t) \\ v_{c2}(t) \\ v_{c2}(t) \end{bmatrix} \tag{16}$$

Where $\nabla = \frac{d}{dt}$

$$K = \begin{bmatrix} L_1 & 0 & 0 & 0 & 0 \\ 0 & L_2 & 0 & 0 & 0 \\ 0 & 0 & C_1 & 0 & 0 \\ 0 & 0 & 0 & C_2 & 0 \\ 0 & 0 & 0 & 0 & l_{load} \end{bmatrix}, a_1 = \begin{bmatrix} 0 & 0 & 1 & 0 & 0 \\ 0 & 0 & 0 & 1 & 0 \\ -1 & 0 & 0 & 0 & 0 \\ 0 & -1 & 0 & 0 & 0 \\ 0 & 0 & 0 & 0 & -R_{load} \end{bmatrix} \text{ and } b_1 = \begin{bmatrix} 0 \\ 0 \\ 0 \\ 0 \\ 0 \end{bmatrix} \tag{17}$$

From the Figure 3(a),state space equation for active states is represented in the form $\nabla x(t) = a_2 x + b_2 u$

$$\begin{bmatrix} L_1 & 0 & 0 & 0 & 0 \\ 0 & L_2 & 0 & 0 & 0 \\ 0 & 0 & C_1 & 0 & 0 \\ 0 & 0 & 0 & C_2 & 0 \\ 0 & 0 & 0 & 0 & l_{load} \end{bmatrix} \nabla \begin{bmatrix} i_{L1}(t) \\ i_{L2}(t) \\ v_{c1}(t) \\ v_{c2}(t) \\ v_{c2}(t) \end{bmatrix} = \begin{bmatrix} 0 & 0 & 0 & -1 & 0 \\ 0 & 0 & -1 & 0 & 0 \\ 0 & 1 & 0 & 0 & -1 \\ -1 & 0 & 0 & 0 & -1 \\ 0 & 0 & 1 & 1 & -R_{load} \end{bmatrix} + \begin{bmatrix} i_{L1}(t) \\ i_{L2}(t) \\ v_{c1}(t) \\ v_{c2}(t) \\ v_{c2}(t) \end{bmatrix} + \begin{bmatrix} 1 \\ 1 \\ 0 \\ 0 \\ -1 \end{bmatrix} V_{in}(t) \tag{18}$$

$$a_2 = \begin{bmatrix} 0 & 0 & 0 & -1 & 0 \\ 0 & 0 & -1 & 0 & 0 \\ 0 & 1 & 0 & 0 & -1 \\ -1 & 0 & 0 & 0 & -1 \\ 0 & 0 & 1 & 1 & -R_{load} \end{bmatrix}, b_2 = \begin{bmatrix} 1 \\ 1 \\ 0 \\ 0 \\ -1 \end{bmatrix} \tag{19}$$

4. TWO PORT QUASI Z-SOURCE INVERTER

Two port battery voltage sources, namely V_{DC1} (lithium battery) and V_{DC2} (fuel cell) is used to drive the EV to achieve better milage and the distance. S_1 to S_9 represents IGBT module connected to the output side of circuit module. These switches provide fast switching response as compared to the n type MOSET for EV module. S_{10} to S_{16} are diodes which are connected to input of circuit module and provide unidirectional flow of current during non-shoot through mode of operation. The combination of L_1, C_1 & L_2, C_2 provides rms voltage which is required for EV operation during shoot through states.

The q-ZSI has been extended in this article with two sources, 9 switches, and bidirectional switches (IGBT'S) is fixed between the load and the source, as illustrated in Figures 4 and 5, depict the basic architecture of the model that has been stated. Figure 5(a), displays the continuous current shoot state with two DC voltage sources, while Figure 5(b), displays a discontinuous current-non shoot through state with a single voltage-fed source. When converting input to output, the aforementioned q-ZSI can perform buck boost operations. The main requirement for EV applications is to reduce switching losses at higher switching frequencies in order to increase efficiency. To V_{peak} and $I_{fundamnetal}$ during 60 degrees of non-switching periods sinusoidal PWM technique is used.
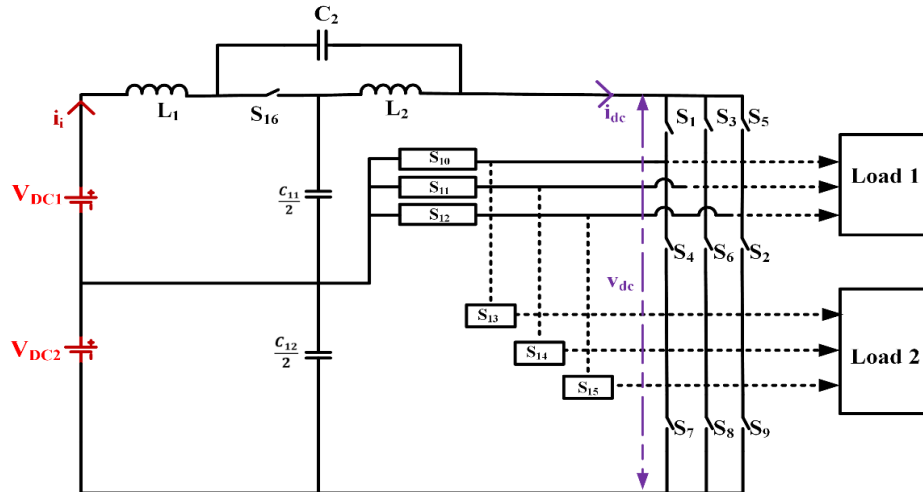
Figure 4. Two port quasi Z source network connected with induction motor load

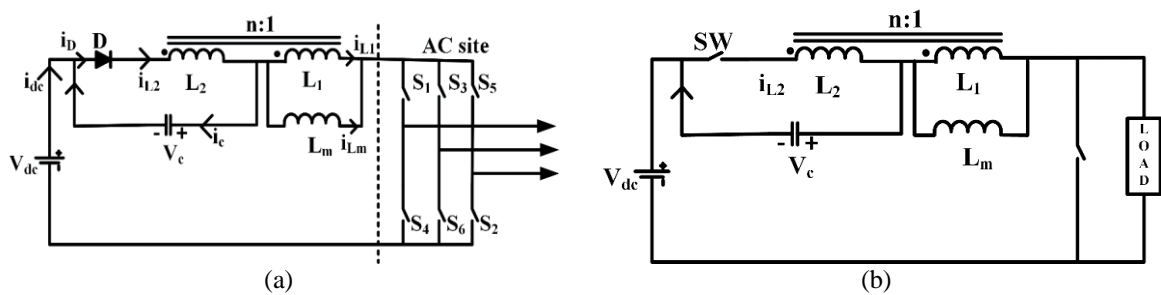(a)   (b)

Figure 5. Two ports quasi-Z source network connected to critical load and non-critical load for; (a) non-shoot through mode and (b) shoot through mode

To produce the gating signal for the switches S_1 to S_7, sine wave is compared to the triangular wave with a reference frequency of 10,000 Hz. Whenever the upper half of triangular wave is greater than upper sine wave, it produces the gating signal for S_1, S_3 & S_5 whereas when lower half of triangular wave is smaller than upper sine wave it produces gating signals for S_7, S_8, & S_9.

$$\frac{d}{dt}\begin{pmatrix} \frac{\Delta i_{L1}}{s} \\ \frac{\Delta i_{L2}}{s} \\ \frac{\Delta v_{C11}(s)}{2}+\frac{\Delta v_{C12}(s)}{2} \\ \Delta v_{C2}(s) \end{pmatrix} =$$

$$\begin{pmatrix} -\frac{1}{L_1(s)} & 0 & \frac{(d-1)}{L_1(s)} & \frac{d}{L_1(s)} \\ 0 & -\frac{1}{L_2(s)} & \frac{d}{L_2(s)} & \frac{(d-1)}{L_2(s)} \\ \frac{(1-d)(s)}{C_{11}+C_{12}} & \frac{d(s)}{C_{11}+C_{12}} & 0 & 0 \\ \frac{d(s)}{C_2} & \frac{(1-d)(s)}{C_2} & 0 & 0 \end{pmatrix} \begin{pmatrix} \frac{\Delta i_{L1}}{s} \\ \frac{\Delta i_{L2}}{s} \\ \frac{\Delta v_{C11}(s)}{2}+\frac{\Delta v_{C12}(s)}{2} \\ \Delta v_{C2}(s) \end{pmatrix} \begin{pmatrix} -\frac{1}{L_1(s)} & (1-d) \\ 0 & (1-d) \\ 0 & (d-1) \\ 0 & (d-1) \end{pmatrix} +$$

$$\begin{pmatrix} \Delta V_{s1}(s) + \Delta V_{s2}(s) \\ i_{dc} \end{pmatrix} \tag{20}$$

$$\begin{pmatrix} \frac{\Delta i_i}{s} \\ \Delta v_{dc}(s) \end{pmatrix} = \begin{pmatrix} \mathbf{1} & \mathbf{0} & \mathbf{0} & \mathbf{0} \\ (\mathbf{1-d}) & (\mathbf{1-d}) & (\mathbf{1-d}) & (\mathbf{1-d}) \end{pmatrix} \begin{pmatrix} \frac{\Delta i_{L1}}{s} \\ \frac{\Delta i_{L2}}{s} \\ \frac{\Delta v_{C11}(s)}{2}+\frac{\Delta v_{C12}(s)}{2} \\ \Delta v_{C2}(s) \end{pmatrix} \tag{21}$$

In (22) presents the small AC signal model of quasi-ZSI

$$\frac{d}{dt}\begin{pmatrix} \frac{\Delta i_{L1}}{s} \\ \frac{\Delta i_{L2}}{s} \\ \frac{\Delta v_{C11}(s)}{2}+\frac{\Delta v_{C12}(s)}{2} \\ \Delta v_{C2}(s) \end{pmatrix} = \begin{pmatrix} -\frac{1}{L_1(s)} & 0 & \frac{(D-1)}{L_1(s)} & \frac{D}{L_1(s)} \\ 0 & -\frac{1}{L_2(s)} & \frac{D}{L_2(s)} & \frac{(D-1)}{L_2(s)} \\ \frac{(1-D)(s)}{C_{11}+C_{12}} & \frac{D(s)}{C_{11}+C_{12}} & 0 & 0 \\ \frac{D(s)}{C_2} & \frac{(1-D)(s)}{C_2} & 0 & 0 \end{pmatrix}\begin{pmatrix} \frac{\Delta i_{L1}}{s} \\ \frac{\Delta i_{L2}}{s} \\ \frac{\Delta v_{C11}(s)}{2}+\frac{\Delta v_{C12}(s)}{2} \\ \Delta v_{C2}(s) \end{pmatrix}+$$

$$\begin{pmatrix} -\frac{1}{L_1(s)} & \frac{(1-D)}{L_1(s)} \\ 0 & \frac{(1-D)}{L_2(s)} \\ 0 & \frac{(D-1)s}{C_1} \\ 0 & \frac{(D-1)s}{C_2} \end{pmatrix}\begin{pmatrix} \Delta V_{s1}(s)+\Delta V_{s2}(s) \\ i_{dc} \end{pmatrix}+\begin{pmatrix} \frac{V_1(s)}{L_1(s)} \\ \frac{V_1(s)}{L_2(s)} \\ \frac{I_1(s)^2}{C_{11}+C_{12}} \\ \frac{I_1(s)}{C_2} \end{pmatrix}(\Delta d)$$

(22)

$$\begin{pmatrix} \frac{\Delta i_i}{s} \\ \Delta v_{dc}(s) \end{pmatrix}\begin{pmatrix} 1 & 0 & 0 & 0 \\ (1-d) & (1-d) & (1-d) & (1-d) \end{pmatrix}\begin{pmatrix} \frac{\Delta i_{L1}}{s} \\ \frac{\Delta i_{L2}}{s} \\ \frac{\Delta v_{C11}(s)}{2}+\frac{\Delta v_{C12}(s)}{2} \\ \Delta v_{C2}(s) \end{pmatrix}+$$

$$\begin{pmatrix} 0 & 0 \\ 0 & -2(1-d) \end{pmatrix}\begin{pmatrix} \Delta V_{s1}(s)+\Delta V_{s2}(s) \\ i_{dc} \end{pmatrix}+\begin{pmatrix} 0 \\ V_2 \end{pmatrix}(\Delta d)$$

(23)

Where: D=duty cycle in steady state, $V_1=v_{C11}+v_{C12}+v_{C2}$, $I_1=i_{dc}-i_{L1}-i_{L2}$, $V_2=-V_1+I_1$,

$X_z=\left[\frac{\Delta i_{L1}}{s} \quad \frac{\Delta i_{L2}}{s} \quad \frac{\Delta v_{C11}(s)}{2}+\frac{\Delta v_{C12}(s)}{2} \quad \Delta v_{C2}(s)\right]^T$ and $U_{1z}=[\Delta V_{s1}(s)+\Delta V_{s2}(s) \quad i_{dc}]^T$

$v_{dc}i_{dc}=v_di_d+v_qi_q=V_{dc\Delta i_{dc}}+I_{dc}\Delta v_{dc}=V_{d\Delta i_d}+I_d\Delta v_d+V_q\Delta i_q+I_q\Delta v_q$

5. RESULTS AND DISCUSSION

Performance test of the conventional ZSIT, conventional trans-ZSI system and proposed two port quasi-ZSI system is implemented using MATLAB/Simulink model. Design parameters are listed in Table 1. Because of the two inductors connected mutually which behaves like transformer in its impedance network, the output of the two port q-ZSI system is often higher. The proposed system was simulated and eventually had a DC link voltage determined using an equation for a modulation ratio of M to 0.85.

Vi=100/(1−(1+2.33)×0.14)=187 V (24)

The AC output voltage's rms value is in the range of 79.42 V (or 112.4 line RMS V), while the load current's rms value is in the range of 7.12 amps.

Table 1. Details MATLAB simulated parameters

Parameters	Notations	Values
Source	VDC	100 V
With dea winding turns	L1	67
Winding turns	L2	47
Coefficient coupling	K	0.99
Mutual inductance	Lm	0.424 mH
Switching frequency	FS	10 KHz
Reference frequency	FR	50 Hz
Modulation index	M	0.85
Resistive load	RL	25 ohm/phase

In oder to prove the concept as stated in section 2, here a MATLAB/Simulink setup has been designed with detail Simulink parameters has been derived based on the load capability of trans-Z source converter. The controllability of the proposed two port quasi trans-ZSI has been tested for EV using step function. This has been done for testing the prototype under actual testing condition. Here an average voltage of 250 V has been

maintained for prototype model in Figure 6. Due to uncontrollable temperature disturbance, there is a overall ripple content of 10% between the hardware and software setup. The hardware setup shows a harmonics varying in between 5.88 to 11.23% based on loading of induction motor at trans-Z source terminal.
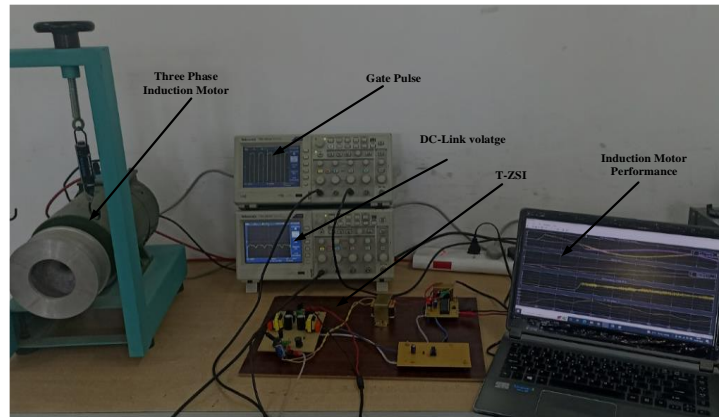

Figure 6. Two port quasi-Z source network with induction motor

Figures 7 and 8 shows the current across the mutual coupled inductors having a value of I_1=28 A, I_1=34 A and V_{cs} (voltage stress across capacitor) is 158.7 V for conventional trans-ZSI whereas for proposed two port quasi-ZSI the voltage stress reduces to 77.02 V with same inductors currents.
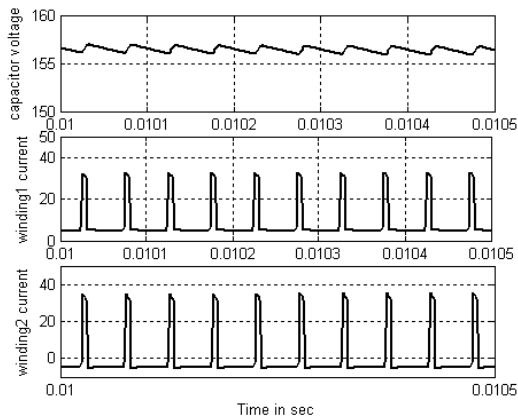
Figure 7. Inductor current 1, inductor current 2 and V_{cs} for conventional trans-ZSI
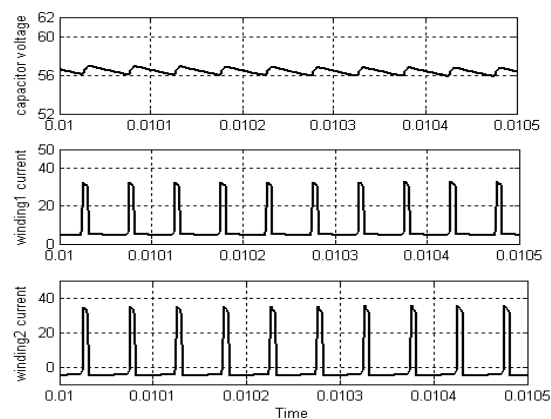
Figure 8. Inductor current 1, inductor current 2 and V_{cs} for two port quasi-ZSI

Figures 9 and 10 shows load current across the motor of I_L=5.7 amp, line -line output voltage across the motor $V_{line-line}$ is 202.2 V, boosted DC voltage of 210 V and the capacitor voltage of 165.7 V for trans-ZSI topology. Having same parameters of the trans-ZSIT, the proposed circuits reduces the voltage stress across by switches by 105.3 V.

In the Figure 11 shows the DC link voltage of 157.7 V, where Figure 12 represents the AC output voltage of 106.78 V and the line current with a value of 7.9 A across the 3-phase load. In Figures 13 and 14 the total harmonics distortion of 5.62% is achieved using MATLAB system and the total harmonics distortion of 6.35% is achieved using hardware module.

Table 2 represent a comparative analysis of THD with a linear load condition. As observed the Z source inverter produces 5.52% of THD with 6 number of switches whereas q-ZSI produces 6.2% of THD with 8 number of switches. With increase in switch level, the THD percentage also increases. However, with the proposed two port quasi-source inverter the total THD present at the output of inverter is 4.96% with nine number of switches.

Similarly at Table 3, shows a comparative analysis of THD with a non-linear load condition is presented where the proposed Z source inverter provides 5.86% of THD with same number of switches. It is also evident

from the discussion that the proposed inverter produces 18.14% extra THD while switching from linear to non linear loading condition which is strictly adhering to International Electricity Code (IEC) code for inverters.
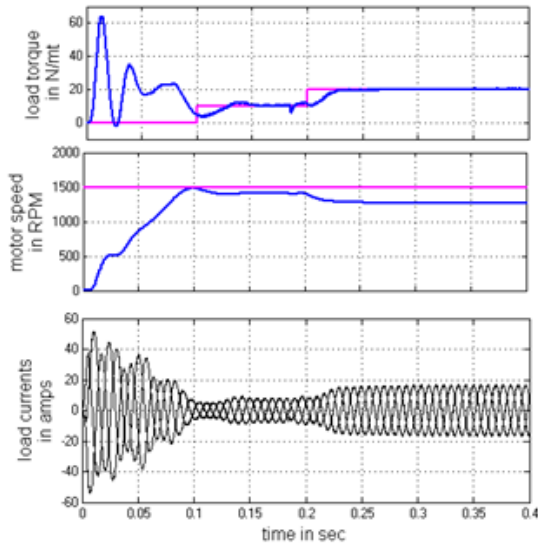

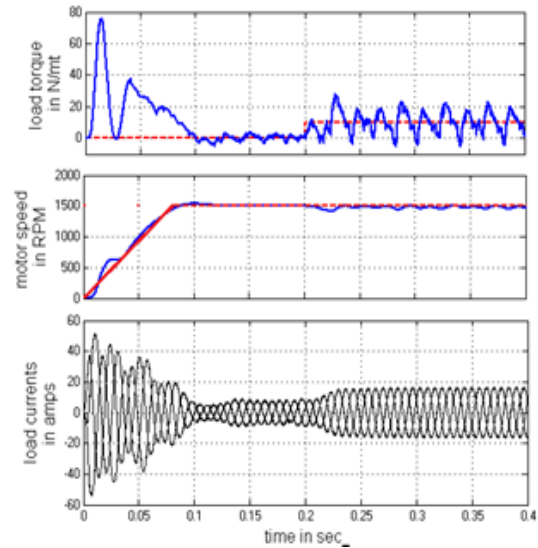Figure 9. Load current, motor speed and torque load of three phase induction motor using trans-ZSI

Figure 10. Load current, motor speed and torque load of three phase induction motor using two port quasi-ZSI
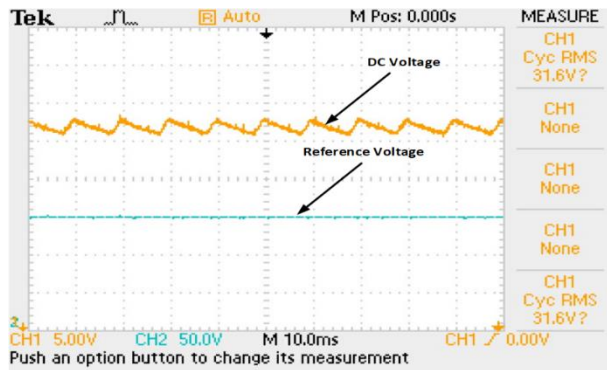

Figure 11. $V_{DC\ ref}$ using MATLAB/Simulink DC link capacitance voltage
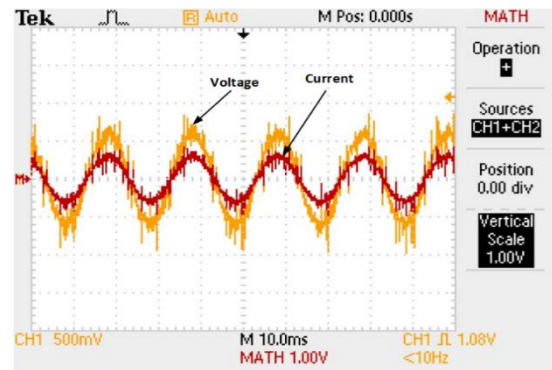
Figure 12. Hardware line to line output AC voltage and line current using hardware module
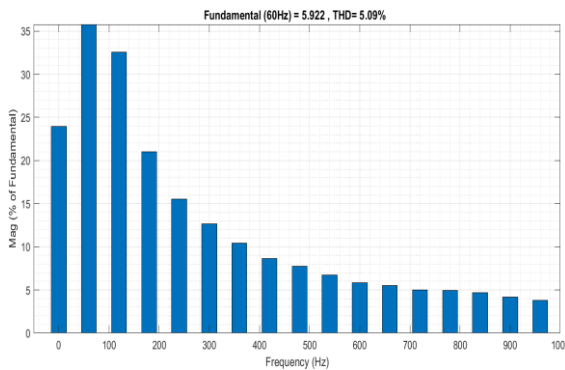

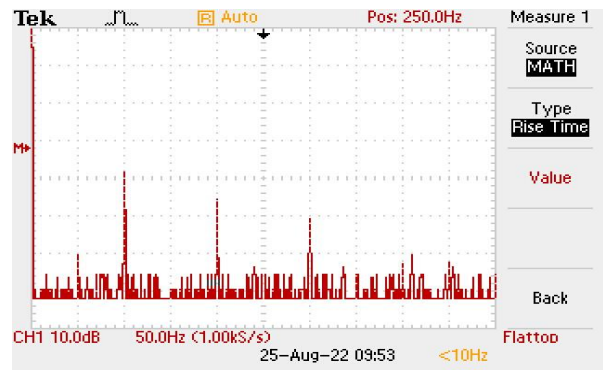Figure 13. Two port quasi-Z network THD analysis using MATLAB/Simulink

Figure 14. Two port quasi-Z network THD analysis using hardware set up

Table 2. A comparative analysis of THD with a linear load condition

Sl. No	Types of Z source network	Number of switches	THD (%)
1	Z source inverter	6	5.52
2	Trans-Z source inverter	6	5.41
3	Quasi-Z source inverter	8	6.21
4	Two port quasi-Z source inverter	9	4.96

Table 3. A comparative analysis of THD with a non-linear load condition

Sl. No	Types of Z source network	Number of switches	THD (%)
1	Z source inverter	6	6.73
2	Trans-Z source inverter	6	6.92
3	Quasi-Z source inverter	8	7.77
4	Two port quasi-Z source inverter	9	5.86

6. CONCLUSION

This research paper compared two various topology of Z-SI. Two port quasi-ZSI and trans-ZSI inverter circuit with initial state and non-initial state of operation is mathematically analyzed and derived. With M=0.85 is used for trans-ZSI and two port quasi-ZSI having resistive load R_L=25 ohm per phase simulated using MATLAB/Simulink software. It has been observed that the voltage stress across capacitor for trans-ZSI topology is much higher than the two port quasi-ZSI topology. Input DC reference voltage of 100 V is used for both the network circuit. It has been observed that for trans-ZSI the DC link voltage is 186.6 V and for two port quasi-Z source networks is 165.5 V. For a fundamental frequency of 60 Hz for proposed topology, 3rd level harmonics is below 4.96% for linear load and 5.86% for nonlinear load in the proposed topology.

REFERENCES

[1]   D. Mande, J. P. Trovão, and M. C. Ta, "Comprehensive Review on Main Topologies of Impedance Source Inverter Used in Electric Vehicle Applications," *World Electric Vehicle Journal*, vol. 11, no. 2, p. 37, Apr. 2020, doi: 10.3390/wevj11020037.
[2]   Y. Tang, S. Xie, and C. Zhang, "An Improved Z-Source Inverter," *IEEE Transactions on Power Electronics*, vol. 26, no. 12, pp. 3865–3868, Dec. 2011, doi: 10.1109/TPEL.2009.2039953.
[3]   K. V. Kumar, R. Reddivari, and D. Jena, "A Comparative Study of Different Capacitor Voltage Control Design Strategies for Z-Source Inverter," *IETE Journal of Research*, vol. 68, no. 2, pp. 1443–1453, Mar. 2022, doi: 10.1080/03772063.2019.1650669.
[4]   Y. P. Siwakoti, F. Z. Peng, F. Blaabjerg, P. C. Loh, and G. E. Town, "Impedance-Source Networks for Electric Power Conversion Part I: A Topological Review," *IEEE Transactions on Power Electronics*, vol. 30, no. 2, pp. 699–716, Feb. 2015, doi: 10.1109/TPEL.2014.2313746.
[5]   W. Qian, F. Z. Peng, and H. Cha, "Trans-Z-Source Inverters," *IEEE Transactions on Power Electronics*, vol. 26, no. 12, pp. 3453–3463, Dec. 2011, doi: 10.1109/TPEL.2011.2122309.
[6]   A.-V. Ho, Ji-Suk Hyun, T.-W. Chun, and H.-H. Lee, "Embedded quasi-Z-source inverters based on active switched-capacitor structure," in *IECON 2016 - 42nd Annual Conference of the IEEE Industrial Electronics Society*, Oct. 2016, pp. 3384–3389. doi: 10.1109/IECON.2016.7793159.
[7]   J. Yuan, Y. Yang, P. Liu, Y. Shen, Z. Qiu, and F. Blaabjerg, "An Embedded Enhanced-Boost Z-Source Inverter," in *2018 IEEE International Power Electronics and Application Conference and Exposition (PEAC)*, Nov. 2018, pp. 1–6. doi: 10.1109/PEAC.2018.8590410.
[8]   J. Yuan, Y. Yang, P. Liu, Y. Shen, and F. Blaabjerg, "An Embedded Switched-Capacitor Z-Source Inverter with Continuous Input Currents," in *2019 IEEE Applied Power Electronics Conference and Exposition (APEC)*, Mar. 2019, pp. 2366–2371. doi: 10.1109/APEC.2019.8722134.
[9]   F. Guo, L. Fu, C.-H. Lin, C. Li, W. Choi, and J. Wang, "Development of an 85-kW Bidirectional Quasi-Z-Source Inverter With DC-Link Feed-Forward Compensation for Electric Vehicle Applications," *IEEE Transactions on Power Electronics*, vol. 28, no. 12, pp. 5477–5488, Dec. 2013, doi: 10.1109/TPEL.2012.2237523.
[10]   H. Torkaman, E. Afjei, A. Keyhani, and M. Poursmaeil, "Control and management of hybrid AC/DC microgrid based on Γ-Z-source converter," *IET Generation, Transmission & Distribution*, vol. 14, no. 14, pp. 2847–2856, Jul. 2020, doi: 10.1049/iet-gtd.2018.6365.
[11]   R. Malathi and M. Rathinakumar, "Comparison of PV based Embedded Z-source inverter fed three phase induction motor with PI controller and PID controller based closed loop systems," in *2017 Third International Conference on Advances in Electrical, Electronics, Information, Communication and Bio-Informatics (AEEICB)*, Feb. 2017, pp. 142–146. doi: 10.1109/AEEICB.2017.7972400.
[12]   R. Reddivari and D. Jena, "Differential mode gamma source inverter with reduced switching stresses," in *2017 IEEE PES Asia-Pacific Power and Energy Engineering Conference (APPEEC)*, Nov. 2017, pp. 1–6. doi: 10.1109/APPEEC.2017.8308937.
[13]   H. Fathi and H. Madadi, "Enhanced-Boost Z-Source Inverters With Switched Z-Impedance," *IEEE Transactions on Industrial Electronics*, vol. 63, no. 2, pp. 691–703, Feb. 2016, doi: 10.1109/TIE.2015.2477346.
[14]   J. Srijeeth, V. C. Thiagarajan, and S. R. Mohanrajan, "Z-Source Dual Active Bridge Bidirectional AC-DC Converter for Electric Vehicle Applications," in *2018 IEEE International Conference on Power Electronics, Drives and Energy Systems (PEDES)*, Dec. 2018, pp. 1–4. doi: 10.1109/PEDES.2018.8707465.
[15]   R. Reddivari, Pruthviraj B G, M. Bharat, and Arjun Kumar G B, "Modified gamma source inverter for fuel cell -battery hybrid electric vehicles," in *2016 Biennial International Conference on Power and Energy Systems: Towards Sustainable Energy (PESTSE)*, Jan. 2016, pp. 1–6. doi: 10.1109/PESTSE.2016.7516518.
[16]   S. Han, H.-G. Kim, B.-G. Gu, H. Cha, T. Chun, and E.-C. Nho, "Induction motor control system using bidirectional quasi-Z source inverter," in *2015 9th International Conference on Power Electronics and ECCE Asia (ICPE-ECCE Asia)*, Jun. 2015, pp. 588–593. doi: 10.1109/ICPE.2015.7167843.
[17]   Y. Tang, S. Xie, C. Zhang, and Z. Xu, "Improved Z-Source Inverter With Reduced Z-Source Capacitor Voltage Stress and Soft-Start Capability," *IEEE Transactions on Power Electronics*, vol. 24, no. 2, pp. 409–415, Feb. 2009, doi: 10.1109/TPEL.2008.2006173.
[18]   T. Senanayake, R. Iijima, T. Isobe, and H. Tadano, "Improved impedance source inverter for hybrid/electric vehicle application

with continuous conduction operation," in *2016 IEEE Applied Power Electronics Conference and Exposition (APEC)*, Mar. 2016, pp. 3722–3726. doi: 10.1109/APEC.2016.7468406.

[19]   F. Z. Peng, "Z-source inverter," *IEEE Transactions on Industry Applications*, vol. 39, no. 2, pp. 504–510, Mar. 2003, doi: 10.1109/TIA.2003.808920.

[20]   S. S, R. C N, S. S. K, J. R. K, R. Dash, and V. Subburaj, "Investigation of Switched Capacitor Multi Level Inverter Topology for Different Voltage Levels," in *2023 4th International Conference for Emerging Technology (INCET)*, May 2023, pp. 1–5. doi: 10.1109/INCET57972.2023.10170352.

[21]   R. Aravind, S. Athikkal, R. E. K. Meesala, K. J. Reddy, R. Dash, and V. Subburaj, "Dual Inductor Based Two Input Two Output DC-DC Converter and its Analysis for DC Microgrid Application," *Distributed Generation & Alternative Energy Journal*, Mar. 2023, doi: 10.13052/dgaej2156-3306.38310.

[22]   S. Saahithi, B. H. Kumar, K. J. Reddy, R. Dash, and V. Subburaj, "Four Speed Auto Transmission DC-DC Converter Control for E-Vehicle and Regenerative Braking Based on Simulation and Model Investigation," *Distributed Generation & Alternative Energy Journal*, Mar. 2023, doi: 10.13052/dgaej2156-3306.38312.

[23]   S. S, R. C N, J. Reddy, R. Dash, and V. Subburaj, "Switched Capacitor MLI Design Ideology with Less number of Switches using Hysteresis Bandwidth Control," in *2022 IEEE International Power and Renewable Energy Conference (IPRECON)*, Dec. 2022, pp. 1–5. doi: 10.1109/IPRECON55716.2022.10059476.

[24]   S. M. Dehghan, M. Mohamadian, and A. Yazdian, "Hybrid Electric Vehicle Based on Bidirectional Z-Source Nine-Switch Inverter," *IEEE Transactions on Vehicular Technology*, vol. 59, no. 6, pp. 2641–2653, Jul. 2010, doi: 10.1109/TVT.2010.2048048.

[25]   J. J. Soon and K. Low, "Sigma-Z-source inverters," *IET Power Electronics*, vol. 8, no. 5, pp. 715–723, May 2015, doi: 10.1049/iet-pel.2014.0274.

[26]   M.-K. Nguyen, Q.-D. Phan, Y.-C. Lim, and S.-J. Park, "Transformer-based quasi-Z-source inverters with high boost ability," in *2013 IEEE International Symposium on Industrial Electronics*, May 2013, pp. 1–5. doi: 10.1109/ISIE.2013.6563650.

[27]   M. Bharat and A. S. R. Murty, "Performance comparison of T-ZSI, ZSI and VSI based on the power loss during switching operation of installed power IGBT switch for EV Applications," in *2022 Trends in Electrical, Electronics, Computer Engineering Conference (TEECCON)*, May 2022, pp. 148–153. doi: 10.1109/TEECCON54414.2022.9854826.

BIOGRAPHIES OF AUTHORS

Manish Bharat (Member, IEEE), Assistant Professor, School of Electrical and Electronics Engineering, REVA University, Holds M.E Degree in "Power Electronics and Drives" from Anna University and B.E degree in Electrical and Instrumentation Engineering from Satyabhama University. Currently he is pursuing Ph.D. under Visvesvaraya Technological University (VTU) Belagavi. He has 12 years of Teaching Experience and 2 years of experience in product development. He has 8 Patents published under IPR, under Government of India. He is active member of IEI, IAENG and IEEE. He has 12 publications in various journals and conferences. His areas of research include Z source inverter and its topology, EV charging, and DC-DC converters. He can be contacted at email: manishb87@gmail.com.

ASR Murty Retd. Professor, Department of Electrical and Electronics Engineering, Rajarajeswari College of Engineering, He completed his M.Tech. in Electrical Engineering on 1978 from IIT Kanpur and Ph.D. in Electrical Engineering on (1997) from IIT Chennai. He worked in Central Power Research Institute, Bangalore as Scitentist Grade V, EO III, EO IV, and joint director used SIMPOW package for power system analysis and developed several tailor made programs in FORTRAN for power system analysis and rendered consultancy services to various electric power utilities. He also handled various subject for U.G and P.G level such as DBMS, programming languages, unix systems programming, theory of computation, C++, Java, signals and systems, digital signal processing, power system operation and amp; control, electric power utilization in various engineering colleges at UG level as a professor. He can be contacted at email: asrmurty1954@gmail.com.

Ritesh Dash (Member, IEEE) was born in Bhubaneswar, Odisha, India, in 1989. He received the Ph.D. degree from the School of Electrical Engineering, KIIT University. He is currently working as an Associate Professor at REVA University, Bengaluru. He has a research experience of over ten years and has sound knowledge in the field of artificial intelligence, FACTS, and machine learning. He has published more than 100 numbers of research papers both in international journals and conferences. Earlier, he has also published a book under CRC press. He has also served the Government of India as a Design Engineer, Electrical at WAPCOS Ltd., A Central PSU under Ministry of Water Resources and Ganga Rejuvenation. He has received Madhusudan Memorial Award and the Institutional Award from the Institution of Engineers, India. He is associated with many international bodies, such as IEEE, Indian Science Congress, The Institution of Engineers, Solar Energy Society of India, and Carbon Society of India. He can be contacted at email: rdasheee@gmail.com.